



FREE CONVECTIVE HEAT TRANSFER CREATED FROM HEATED CYLINDER IMMERSSED INSIDE DUCT COOLED FROM SIDE

Qais Abid Yousif^a, Omar Rafae Alomar^{a,*}, Obed M. Ali^b, Omar Mohammed Ali^c

^a Northern Technical University, Engineering Technical College of Mosul, Cultural Group Street, Mosul, 41002, Iraq

^b Northern Technical University, Technical Institute Alhujja, Kirkuk, 36001, Iraq

^c University of Zakho, Collage of Mechanical Engineering, Kurdistan Region, 42002, Iraq

ABSTRACT

This work involves a numerical investigation on free convection heat transfer occurred by a hot cylinder immersed in a square duct cooled from one side under different temperatures. Simulations have been done for a large ranges of Rayleigh number ($10^3 \leq Ra \leq 10^7$) and right wall temperature ($0 \leq T_r \leq 0.75$). The results displayed that Nu is enhanced with rising in Ra and decreasing in T_r . The value of Nu is decreased with rising in T_r , where the maximum reduction in Nu is about 32% for $T_r=0.75$ as compared to $T_r=0$. The maximum enhancement range for Nu is found between 50% and 100% for low Ra and between 20% and 30 % for high Ra . The variations of local Nu display that Ra has an extremely actions on the characteristics of flow and temperature fields.

Keywords: *different side cold wall temperature, free convection, single hot cylinder, enclosed duct.*

1. INTRODUCTION

Natural convective heat transfer created inside duct having heated cylinders has become interested subject due to their wide applications in different engineering fields such as aircraft cabin insulations, solar collectors, thermal storage systems, and cooling systems of nuclear reactors (Ali, O., (2014), Nada and Said (2019), Webb and Itamura (2003), Talesh Bahrami and Safikhani (2020)). Several investigations deals with free convective induced from cylinder have been presented by several authors using different methods (Kahwaji et al. (2012), Kahwaji et al. (2011), Ali et al. (2014), Kahwaji et al. (2013), Ali and Mahmood (2020), Ali et al. (2022)).

Shu et al. (2001) numerically studied the free convective eccentric annulus positioned horizontally between a heated inner and outer cylinders using the method of differential quadrature (DQ). The outcomes have been compared with the available data from previous studies to validate the used method in which very good agreement has been obtained. Kim et al. (2014) presented a study on free convective inside a duct having a cylinder using the immersed boundary method at a 0.7 Prandtl number under various Rayleigh number (Ra). In their study, they focused on the influence of changing the lower duct surface temperature on the characteristics of free convective. With increasing Ra , the streamlines and isotherms variations has been also increased, which in turn, increases the variation in the number of convective cells formation inside duct. Moreover, they observed that the Nusselt number distribution at cylinder wall, top and bottom wall of the enclosure depends on Ra and temperature of bottom wall. Yoon and Shim (2021) investigated numerically the natural convection at a 0.7 fixed Prandtl

number and three Ra of 10^3 , 10^4 and 10^5 from a hot cylinder inserted inside a cold duct. In this study, the flow structures have been classified according to the position of the cylinder. Accordingly, a map for the flow structures has been provided in this study at each Ra and four structures flow modes have been observed and mainly divided by big inner and circulation vortices for the cases of Ra equal to 10^3 and 10^4 . The first mode that existed at $Ra = 10^3$ and 10^4 disappeared when $Ra = 10^5$ from the flow structures map. On the other hand, the three new modes observe at $Ra = 10^5$, resulting in total six flow structures modes have been characterized by the top side secondary vortices. Nabavizadeh et al. (2012) presented the laminar free convection in a cold inner sinusoidal circular cylinder inside a hot outer square enclosure at different angles, amplitudes and undulations number. In their study, both cylinder and square enclosure which filled by air have been kept at constant temperature. The computed solutions displayed that the increasing in number of undulations or amplitude or changing the angle results in changing the coefficient of heat transfer and has a noticeable effect on the fluid fields and temperature. Kuscu et al. (2015) numerically presented natural convection inside enclosure cooled by peltier impact. In this study, the top and bottom walls have been considered adiabatic, whereas the left vertical wall has been kept at fixed constant heat flux and the right vertical wall has been subjected at cold temperature. The obtained results displayed the thermal plume has been developed at the lower left part of the duct in the early stage of the flow.

Sheikholeslami et al. (2013) numerically investigated the effect of using magnetic field on natural convection induced inside a curved-shape enclosure under different values of Rayleigh number and Hartmann

* Corresponding author. Email: omar.alomar@ntu.edu.iq

number. The results indicated that the Nusselt number has been decreased with increasing in Hartmann number. Sheikholeslami et al. (2014) presented a numerical study on the impacts of free convection induced from a heated elliptical duct inserted inside a cold circular duct using Cu-water nanofluid as a working fluid. The results showed that the Nusselt number has been increased with rising in inclination angle, Rayleigh number and volume fraction of nanoparticle. Furthermore, it has been found that the increase in Rayleigh number leads to decrease the enhancement in heat transfer. Hussain, S. H. and, Hussein, A. K. (2011) numerically studied the free convection in a differentially heated duct with heat generating conducting circular cylinder at various diagonal positions. The results indicated that the Rayleigh number and heat generation have a clear influence on the flow and heat fields, whereas the locations of inner cylinder locations has no nearly influence when the inner cylinder does not generate heat. Atayilmaz and Teke (2009) experimentally and numerically studied the free convection from a horizontal cylinder for purpose of comparison. The numerical results and experimental data fall in $\pm 20\%$ band. Ghaddart (1992) numerically analyzed the natural convection from a heated horizontal cylinder inserted inside rectangular duct. The results show that the optimal rate of heat transfer out of the duct happen at the upper surface. Sheikholeslami et al. (2012) numerically studied the natural convection of Cu-water nanofluid in a cold outer circular duct having a heated sinusoidal cylinder with a magnetic field. The solutions indicated that the enhancement ratio has been reduced with rising in Rayleigh number in the absence of magnetic field, whereas a reverse trend has been found with adding the magnetic field. Saleh et al. (2015) numerically investigated the free convection occurred inside cold polygonal duct having a heated inner circular cylinder. The results showed that the polygonal shape has no influence to the Nusselt number distribution. Billah et al. (2011) numerically analyzed the mixed convection in a lid-driven cavity having a hot circular hollow cylinder immersed at the center of the cavity. The results displayed that the velocity and temperature profiles are strongly depend on the solid-fluid thermal conductivity ratio and cylinder diameter. Kim et al. (2014) numerically presented the results of immersed boundary method of free convection inside duct having an inner circular cylinder. The results indicated that the variations in velocity and temperature are strongly depend on the bottom wall temperature and Rayleigh number. Al-Jabair, S. and Habeeb, L. J., (2012) numerically simulated the performance of free convection inside a cold outer inclined square duct having a hot circular cylinder. The solutions displayed that the Rayleigh number and aspect ratio are critical to the behaviors of heat and flow fields. Furthermore, the angle of inclination has a nominal action on heat transfer for all Ra . Sravanthi, P.M. and Madhavi, M.R., (2022) numerically studied the reaction of magnetic field and activation energy of nanofluid gyrotactic microorganisms assuming viscous dissipation condition. In their study, the action of several factors on Nusselt number and density number of motile microorganisms are presented. Nagalakshmi, P.S.S. and Vijaya, N., (2022) numerically tested the entropy generation of the spatial temporal state of nanofluid between two plates. The findings display that the entropy generation can be decreased with rising Fourier's number in nanofluids. Ganesh, G. R. and Sridhar, W., (2021) numerically studied the characteristics of heat flied of MHD Casson fluid by involving the radiation effect and chemical reaction over permeable stretching sheet. The outcomes indicated that the heat transfer rate reduces with increasing in magnetic parameter. In addition, for progressive values of radiation parameter and hall parameter, the heat transfer rate increases as chemical reaction parameter is decreased.

To control and enhance the mechanism of free convection heat transfer inside enclosed duct, the general remedy that can be used with free convection magnification is employing a single heated cylinder. A survey on the previous studies confirm that a large fascinating are given to display the mechanism of mixed convective that induced from a single hot cylinder located in a ventilated duct. Moreover, the survey on the previous research works illustrate that the works that assumed free convection in presence of a single circular in an enclosed duct cooled from one vertical surface are very limited. The used of heated cylinder aimed to control the structures of heat and flow fields of free convective inside duct and hence, this case leads to convective inhibition. To have a complete vision on the actions of free convective, a detailed solutions are required. Thereby, the aims of the current study is to analyse numerically the free convective occurred by single hot cylinder located inside a square enclosed duct only cold from only right vertical side. Actions of a large range of Ra ($10^3 < Ra < 10^7$) and right wall temperature (T_r) on the isotherms and streamlines are displayed and discussed. The behaviour of Nusselt number is also displayed in the current work.

2. PHYSICAL PROBLEM AND THEORETICAL MODEL

2.1 Physical Problem

The current schematic configuration is given in Fig. 1(a), which represents a hot cylinder immersed inside an enclosed square channel. The cylinder has a diameter (d) equal 5cm and the enclosure width (L) equal 20cm and hence, the duct width to the cylinder diameter ratio (L/d) is equal 4. The circular cylinder has been subjected at high temperature and immersed in the middle of duct. The lower, upper, and left surfaces of duct have been selected to be adiabatic, whereas the right surface has been considered to be at various low temperature (T_r). The enclosure has been filled by air.

2.2 Mathematical Model

In the present work, the energy and Navier-Stokes equations have been utilized to predict and describe the thermal and flow behaviors inside the duct (Webb et al. (2003) and Ansys, I., (2018)). The governing equations has been set under laminar flow, constant properties and steady-state conditions. Thus, the governing formulation can be presented in dimensionless form as Karimi et al. (2016):

$$\frac{\partial u}{\partial x} + \frac{\partial v}{\partial y} = 0 \quad (1)$$

$$U \frac{\partial U}{\partial X} + V \frac{\partial U}{\partial Y} = -\frac{\partial P}{\partial X} + Pr \left(\frac{\partial^2 U}{\partial X^2} + \frac{\partial^2 U}{\partial Y^2} \right) \quad (2)$$

$$U \frac{\partial V}{\partial X} + V \frac{\partial V}{\partial Y} = -\frac{\partial P}{\partial Y} + Pr \left(\frac{\partial^2 V}{\partial X^2} + \frac{\partial^2 V}{\partial Y^2} \right) + RaPrT \quad (3)$$

$$U \frac{\partial T}{\partial X} + V \frac{\partial T}{\partial Y} = \left(\frac{\partial^2 T}{\partial X^2} + \frac{\partial^2 T}{\partial Y^2} \right) \quad (4)$$

where the dimensionless parameters are given as follows:

$$X = \frac{x}{L}, Y = \frac{y}{L}, U = \frac{u}{u_i}, V = \frac{v}{u_i}, P = \frac{p}{\rho u_i^2}, T = \frac{T - T_f}{T_c - T_f} \quad (5)$$

For natural convection, the fluid density changes owing to temperature change and hence, the buoyancy force represents the dominant term. The buoyancy depends on the enclosure width L and its intensity can be displayed by Rayleigh number (Ra) and thus, Ra can be written as follows:

$$Ra = \frac{g\beta\Delta TL^3\rho}{\mu\alpha} \quad (6)$$

where $\alpha = \frac{k}{\rho c_p}$ and $\beta = \frac{-1}{\rho} \left(\frac{\partial \rho}{\partial T} \right)_p$ are the thermal diffusivity and thermal expansion coefficient.

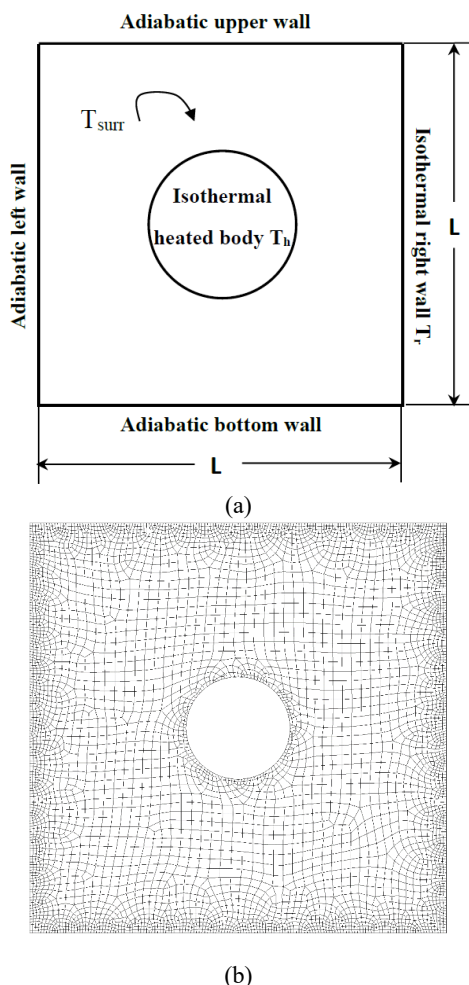


Fig. 1 Schematic representation of (a) cylinder-duct combination and (b) grid distributions of current problem

3. NUMERICAL ALGORITHM AND GRID INDEPENDENCE STUDY

In the current work, finite volume approach has been utilized to solve Eqs. (1) – (4) by using a software ANSYS Fluent package. Second order upwind method has been employed for the discretization of energy, pressure and momentum. For conservation of momentum, the Boussinesq relationship has been taken into account during the simulations. In addition, the properties of the fluid inside the duct have been evaluated according to the average temperature at cylinder surface and mean air temperature. The simple algorithm approach has been employed to solve momentum equation. To solve the governing equations, a grid distribution has been generated to ensure the optimum size of grid as presented in Fig. 1(b). In the present study, a hexagonal shape cell has been used. Different number of cells have been examined to ensure the grid independence solutions at $Ra = 5 \times 10^6$ and the results are illustrated in Table 1. The solutions in Table show that the mesh (no. of nodes and elements of 11,611 and 11,901) generate independent solution and thus, this number of cells have been used for simulations. The convergence criteria of energy, momentum and continuity has been chosen to be 10^{-6} to reach a convergence solution.

Table 1 Mesh independency test for $Ra = 5 \times 10^6$ and $L = 4$

Number of cells (Nodes)	11,901 (11,611)	19656 (19371)	37101 (36828)	76613 (76406)	149230 (149066)
Nu	8.08271	8.08975	8.04730	8.0422	8.021128

4. VALIDATION PROCESS

The current numerical model has been examined through comparing the present solutions with previous numerical and experimental solutions.

4.1 Numerical Validation

The problem under validation is the free convective created by a single hot cylinder inserted in an enclosed square duct. The ratio of duct length to diameter of cylinder (L/d) equal 4 with Ra values of 10^4 , 10^5 and 10^6 has been compared with numerical results which obtained by Shu, C. and Zhu, Y. D. (2002). The comparison has been done under the same configuration, operating parameters and boundary conditions and displayed in terms of Nu , streamlines and isotherms as illustrated in Fig. 2(a) and Table 2. The agreements of the streamlines and isotherms between two studies is very good, where the maximum difference of the average Nu is about 6%.

4.2 Experimental Validation

The current results of Nusselt number has been also validated against experimental data that presented by Ali, O. (2008). The problem under validation is the natural convection induced from different cross section cylinders in a vented enclosure. The comparison is presented in Fig. 2(b) for various Ra and $L/d=2.5$. The comparison has been done under the same configuration, operating parameters and boundary conditions and displayed in terms of Nu . The agreements of Nu between two studies is very good, where the maximum difference of the average Nu is about 8%

Table 2 Comparisons between present Nusselt numbers with previous results of Shu and Zhu (2022)

Ra	Nu	
	Present	Results of Shu and Zhu (2022)
10^4	3.0578	3.24
10^5	4.7655	4.86
10^6	8.6899	8.9

2.3 Boundary Conditions

To solve the conservation equations, the following boundary conditions have been used:

I) At the surface of cylinder;

$$T_c = 1 \quad (7a)$$

$$U = 0 \quad (7b)$$

$$V = 0 \quad (7c)$$

II) At the upper, lower and left surfaces of duct;

$$\frac{\partial T}{\partial X} = 0 \quad (8a)$$

$$V = 0 \quad (8b)$$

$$U = 0 \quad (8c)$$

III) At the right surface of duct, a variable non-dimensional temperature has been used as follows:

$$T_r = 0, 0.25, 0.5, 0.75, 1 \quad (9a)$$

$$V = 0 \quad (9b)$$

$$U = 0 \quad (9c)$$

2.4 Average Nusselt Number (Nu_{av})

In the current study, Nu_{av} at cylinder wall has been obtained by integrating the following relationship;

$$Nu_{av} = \frac{h_{avg}D}{k} = \frac{-1}{2\pi} \int_0^{2\pi} \frac{\partial T}{\partial n} \quad (10)$$

In Eq. (10), h_{avg} displays the average heat transfer coefficient and k displays the air thermal conductivity (Ali et al. (2021) and Alomar et al. (2023)).

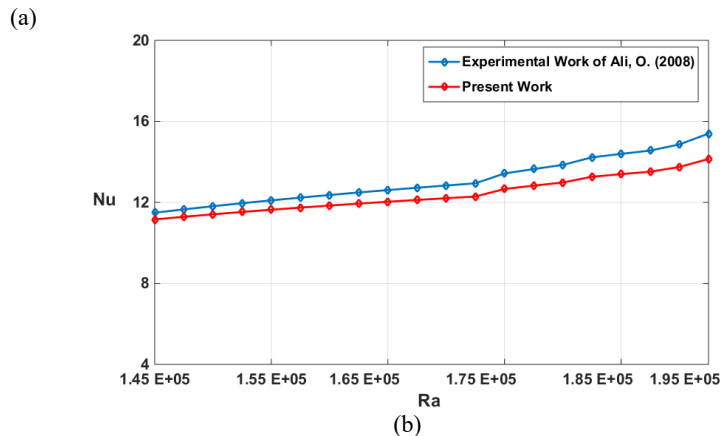
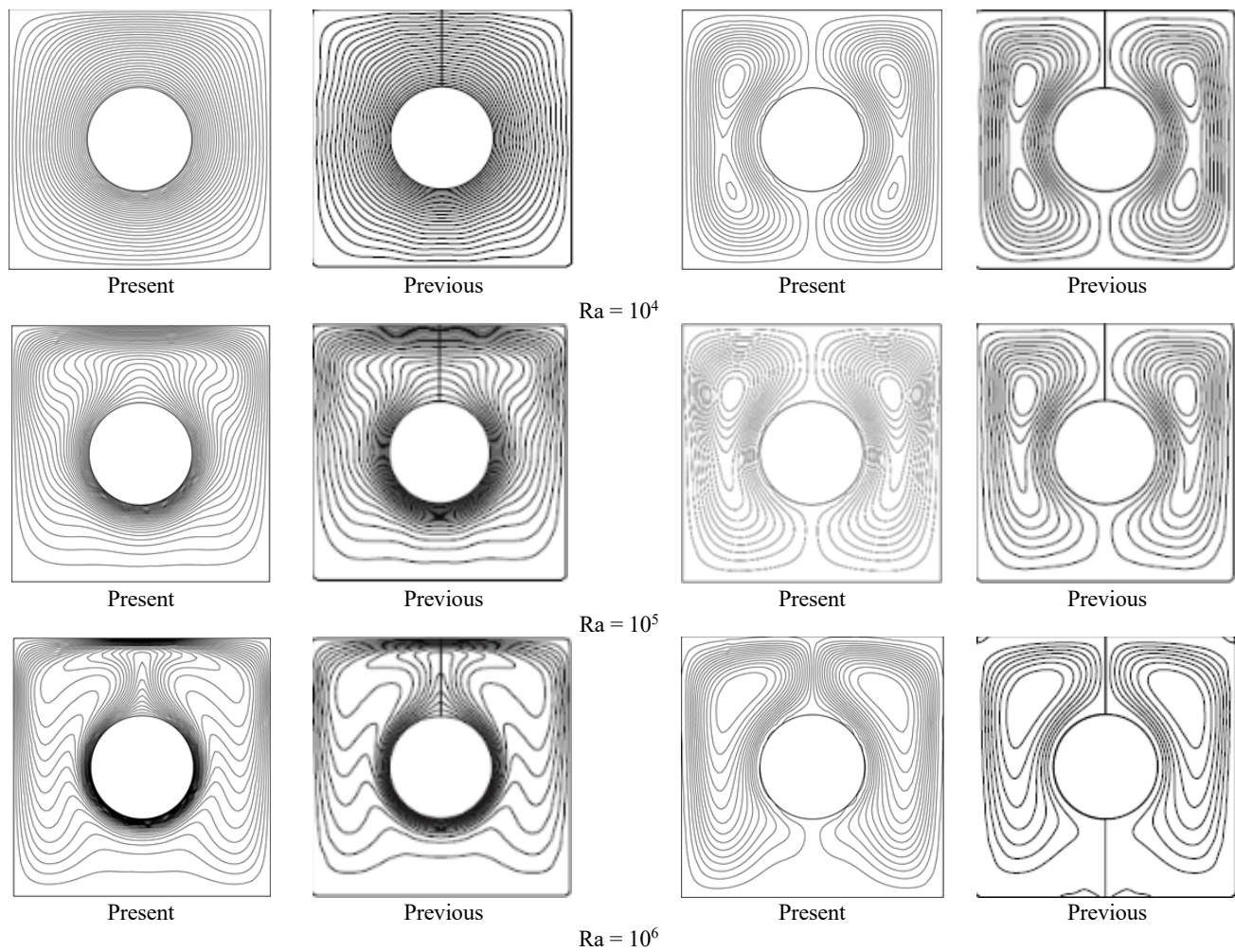


Fig. 2 Validation of (a) the current results and the numerical solutions of Shu and Zhu (2002) for various Ra and (b) present Nu and experimental solutions of Ali, O. (2008) for various Ra

5. RESULTS AND DISCUSSION

5.1 Isotherms and Streamlines Fields For $Tr = 0$

Figure 3 illustrates the distributions of streamlines and isotherms inside the computational domain when the right wall temperature $T_r=0$ for various Ra . Due to the buoyancy force the hot fluid moves towards upper direction (above of cylinder). The flow has been directed to the right wall of duct due to all other surfaces have been considered to be adiabatic. When the fluid reaches the cold wall, it becomes slowly denser and colder and hence, the denser cooled fluid moves directly towards the bottom surface. As Ra is increased, the heated fluid moves upward

towards the top surface. Thus, the main circulation of flow is appeared. When $Ra = 10^3$, the convection is mainly developed by quasi-heat conduction because the velocity of fluid is low as displayed in the isotherms contour lines in Fig. 3. The parallel vertical cooled isotherms lines have been appeared along the right duct surface and the fluid is heated as moves towards the cylinder. The solutions in Fig. 3 show two symmetric pattern due to the impacts of buoyancy is very weak. As Ra is raised to 10^4 , the symmetric pattern of the main flow has been slightly changed and an inner vortex has been created close to the right side of cylinder. The parallel cooled isotherms lines become thinner and a single

upwelling plume occurs above the top side of cylinder towards the upper wall of duct. A thick thermal layer around the bottom side of the cylinder has been displayed. As Ra is continues raised to 10^5 , the main flow circulation becomes non symmetrical and the cooled fluid moves towards the right side of duct, which replaces with a hot fluid around the cylinder and hence, the shape of the cooled vortex is changed. As a result, the heat transfer above the cylinder is dominant by convection flow, where the temperature gradient is strong. At this Ra value, the thickness of the upwelling plume above the top surface of the cylinder become thinner. At $Ra = 10^6$, the heat is generally transferred by convective. Since the fluid velocity is extremely increased with enhancing in Ra , the behavior of boundary layer has been presented at the left part of cylinder. Thus the

shape of the cooled vortex has been modified. The stratified layers that developed inside the duct are represented by cold layer at the bottom surface of duct and hot layer at the upper surface of duct. It can be observed that the thickness of thermal boundary layer has been decreased around the cylinder as shown for the solution at $Ra = 10^6$. As a results, the flow is extremely impinged at the upper surface of duct. As Ra is increased to 10^7 , the fluid velocity is considerably raised which leads to enhance the main flow circulation inside the enclosure. Moreover, the thickness of thermal boundary layer has been sharply decreased and the thickness of thermal plume at the top surface of the cylinder has been extremely reduced.

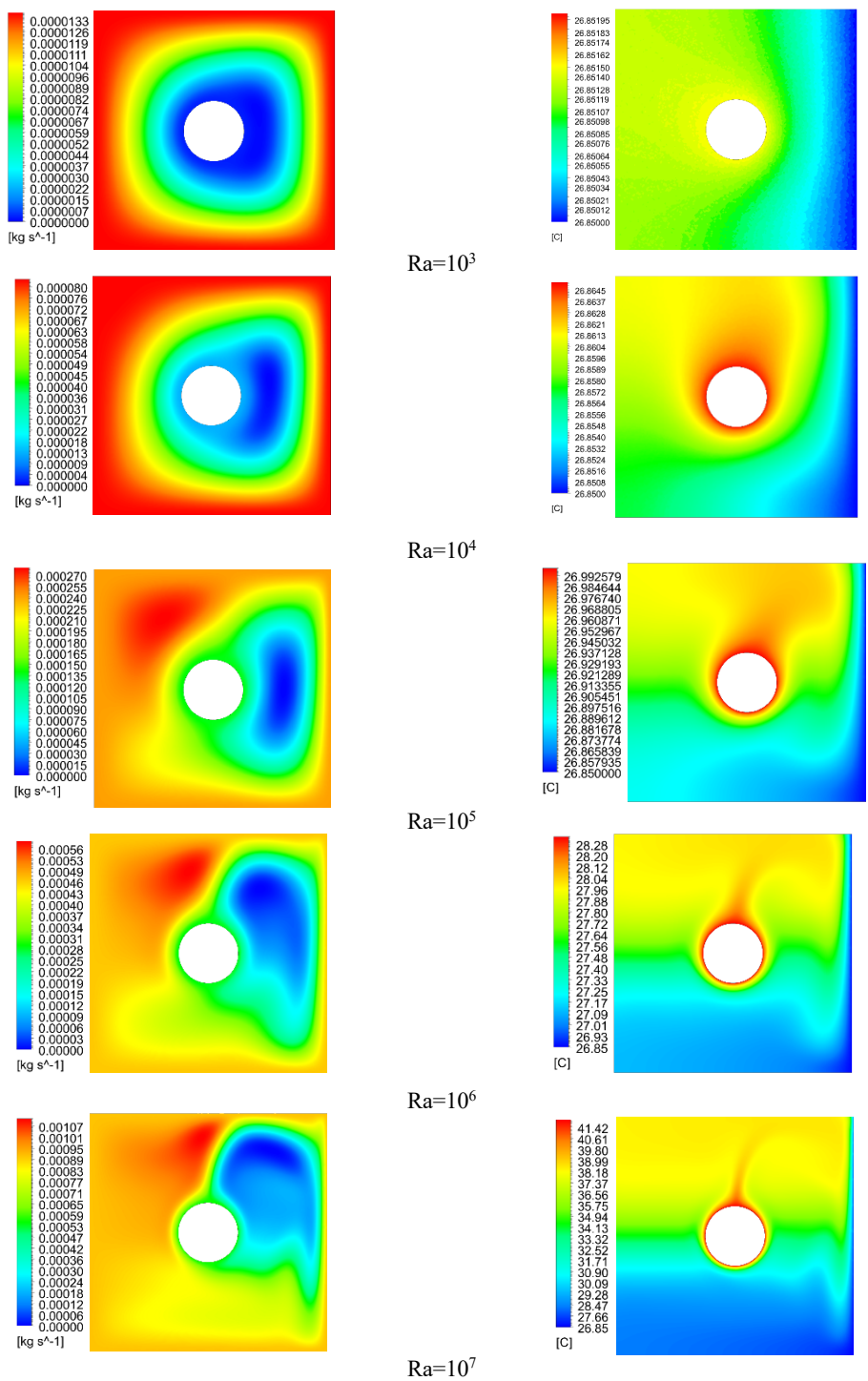


Fig. 3 Solutions of isotherms and streamlines for various Ra at dimensionless right wall temperature $T_r = 0$

5.2 Effects of various Right Side Cold Temperature (T_r)

The distributions of isotherms and streamlines at $Ra = 10^3$ for different values of T_r is given in Fig. 4. As shown from this figure, the variation in T_r has a small action on the overall flow structure. For $T_r = 0$ and 0.5, two fold symmetric patterns in the main circulation have been appeared. For $T_r = 0.75$, the difference in temperatures between cylinder and T_r of duct is very low and hence, therefore there is no convection heat transfer between two surfaces. Moreover, the isotherms layers are parallel to the right wall of duct. The structure of the isotherms contour lines is changed as T_r is increased due to shrink in the temperature gradient near the cylinder wall. Figure 5 shows the distributions of streamlines and isotherms at $Ra = 10^4$ under various T_r values. The results in Fig. 5 display that the increasing in Ra leads to enhance the flow velocity and rise the depth of thermal layer. The thermal structure changes and a thermal plume is directed towards the left upper corner of the enclosure when T_r is increased. As Ra is increased to 10^5 , the solutions in Fig. 6 show that there is a minor difference in the structures of flow and hence, the change in T_r has only a minor influence. It can be also observed from Fig. 6 that the contribution of convection is increased. The flow velocity has been decreased as T_r is increased due to decrease the difference in temperature between cylinder and T_r . Furthermore, a single cooled vortex core is formed between the cylinder and right side of the enclosure. Moreover, the thermal boundary thickness has been increased with increasing in T_r . A thermal plume also forms above the top surface of cylinder, where its thickness decreases with rising in T_r . As Ra is further increased to 10^6 , the results

in Fig. 7 display that the action of convective is the dominant mode for all values of T_r . The flow velocity has been increased as compared to those obtained with $Ra = 10^5$. For this Ra value, however, the flow velocity has been decreased with rising in T_r . In this case, the shape and location of the single cooled vortex core have been changed as compared to the solutions that obtained for $Ra = 10^5$. Also, the length of the vortex has been expanded as T_r is raised. The depth of thermal layer has been increased due to decrease in temperature difference between cylinder and right surface of duct. Based on the value of Ra in this case, the depth of thermal layer and the upwelling thermal plume above the cylinder have been decreased as compared to those obtained for $Ra = 10^5$. Moreover, the depth of both thermal layer and the upwelling thermal plume have been expanded as T_r is increased. As Ra is continuous increased to 10^7 , the value of flow velocity inside the enclosure has been increased as compared to previous cases of Ra . On the other hand, the flow velocity has been reduced as T_r is increased for this Ra value. The shape and location of the single cooled vortex core is also changed as compared to the case of $Ra = 10^6$. However, the results show that T_r has only a minor effect on vortex shape, whereas the boundary layer thickness has been enhanced as T_r is raised. The depth of thermal layer and the width of upwelling thermal plume above the cylinder have been reduced as compared to those obtained for $Ra = 10^6$. As T_r is increase, the results in Fig. 8 indicate that the depth of both thermal layer and the upwelling thermal plume have been raised

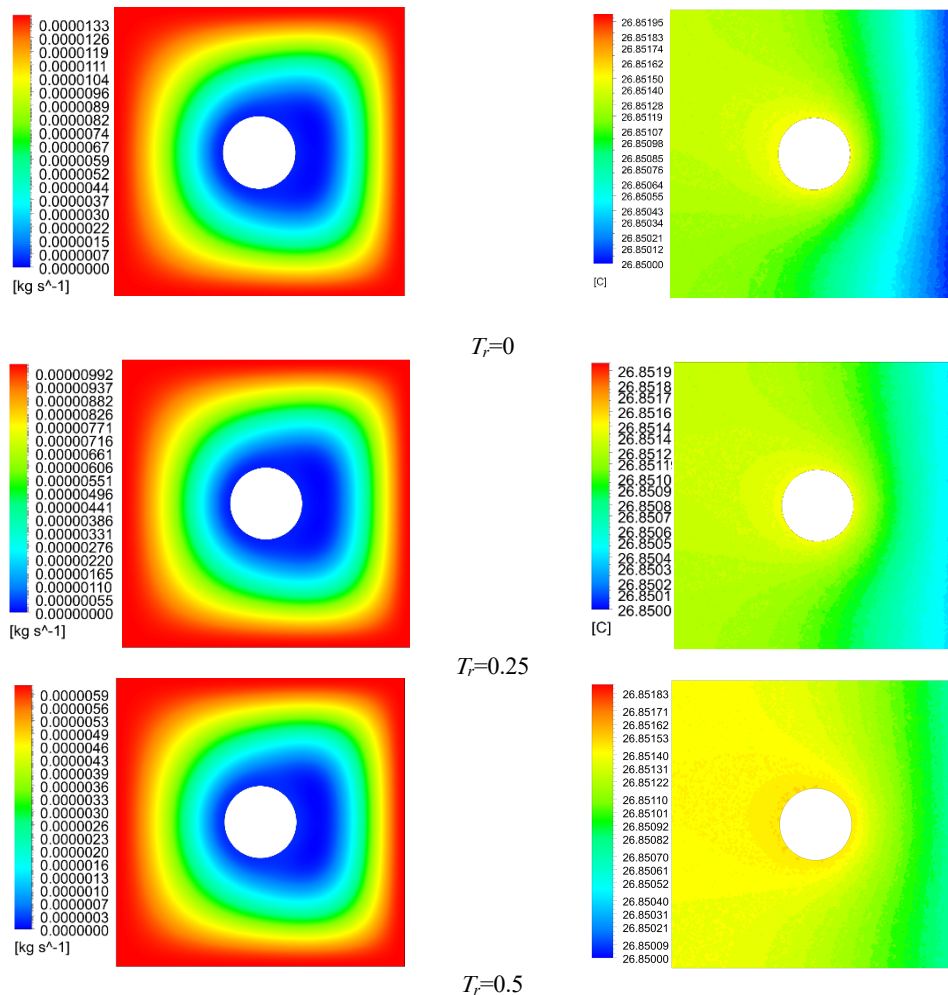


Fig. 4 Solutions of isotherms and streamlines for various T_r at $Ra = 10^3$

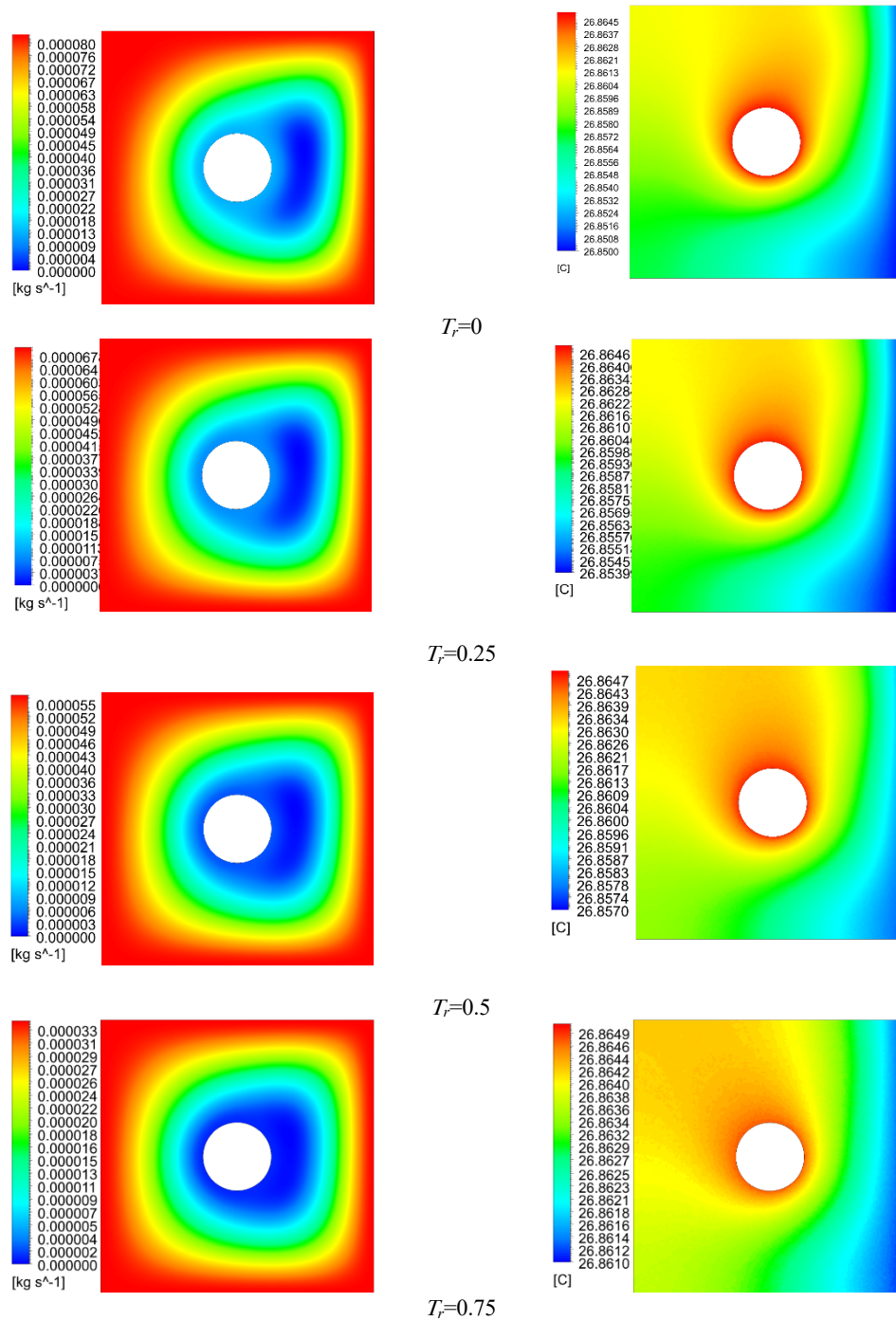


Fig. 5 Solutions of isotherms and streamlines for various T_r at $Ra = 10^4$

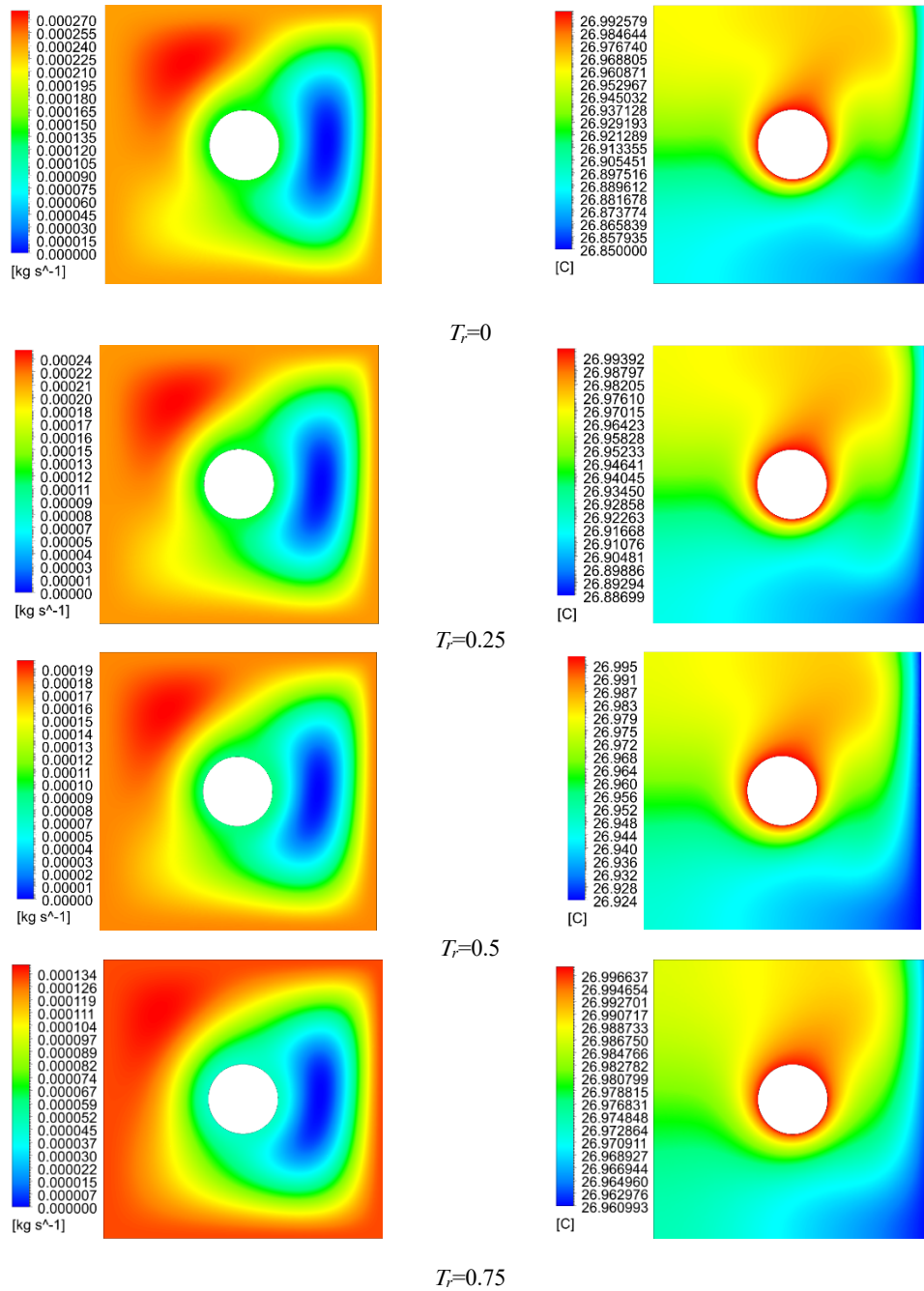


Fig. 6 Solutions of isotherms and streamlines for various T_r at $Ra = 10^5$

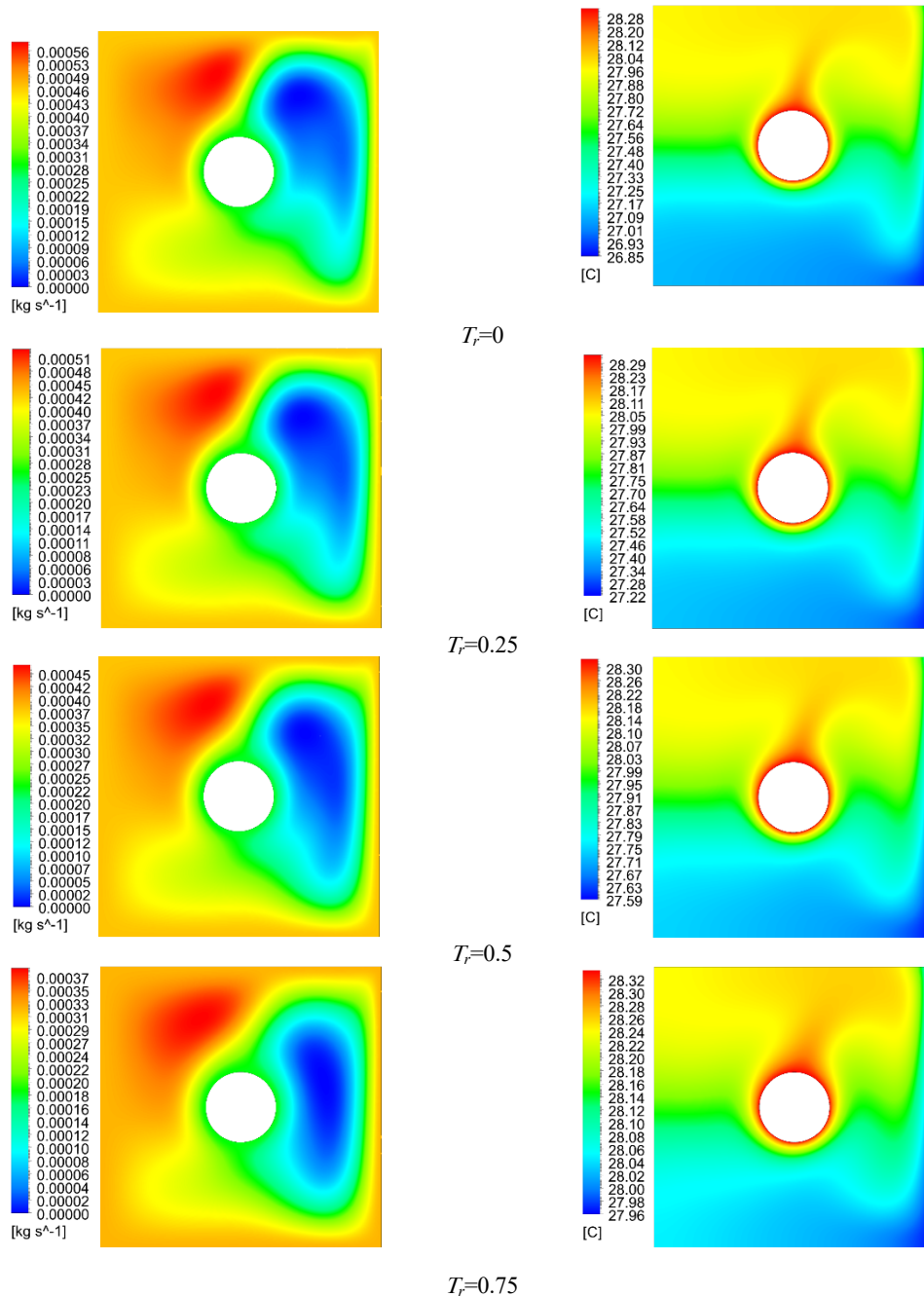


Fig. 7 Solutions of isotherms and streamlines for various T_r at $Ra = 10^6$

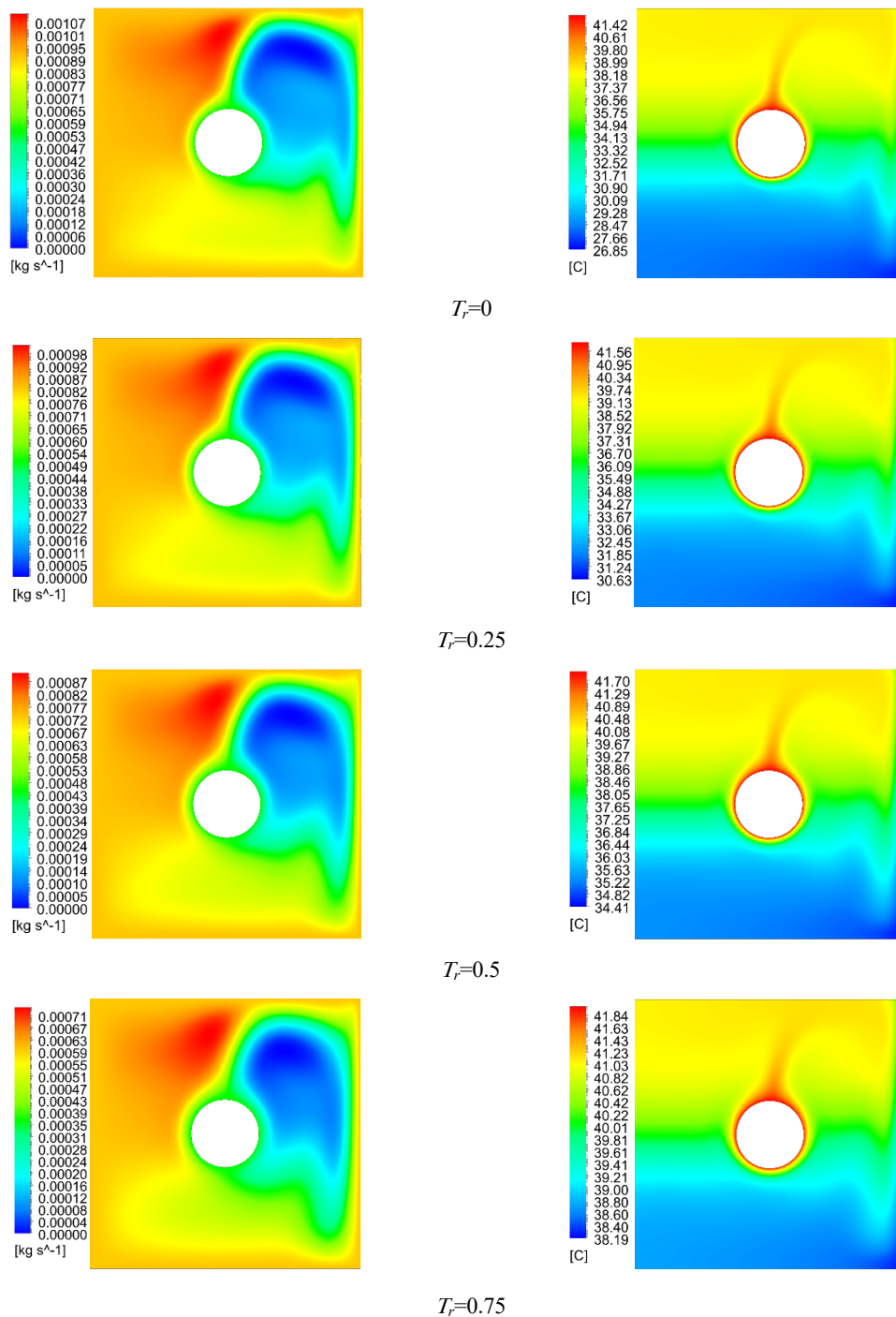


Fig. 8 Solutions of isotherms and streamlines for various T_r at $Ra = 10^7$

5.3 Solutions of Local Nusselt Number

The variations of Nu_{cyl} along the cylinder surface for various values of Ra and T_r is illustrated in Fig. 9. The results confirm that the minimum values of the Nu_{cyl} have been obtained at the angle degree of 0° , 60° , 120° , 240° , 300° and 360° , respectively. For $Ra = 10^3$ and $T_r=0$, the smallest Nu_{cyl} value has been observed at angle of 90° (right stagnation point of cylinder). At $T_r=0$, the variations in the values of Nu_{cyl} according to the angle is low when the heating from right surface

is absent at $Ra = 10^3$. As T_r is increased, Nu_{cyl} has been reduced due to rise the air temperature in the right side of cylinder. The Nu_{cyl} values have been increased with increasing in Ra . For medium and high values of Ra ($Ra > 10^4$), the maximum values of Nu_{cyl} have been observed at the angles ranging between 150° and 210° due to the influence of buoyance force. The results also displayed that Nu_{cyl} values have been decreased as T_r is increased.

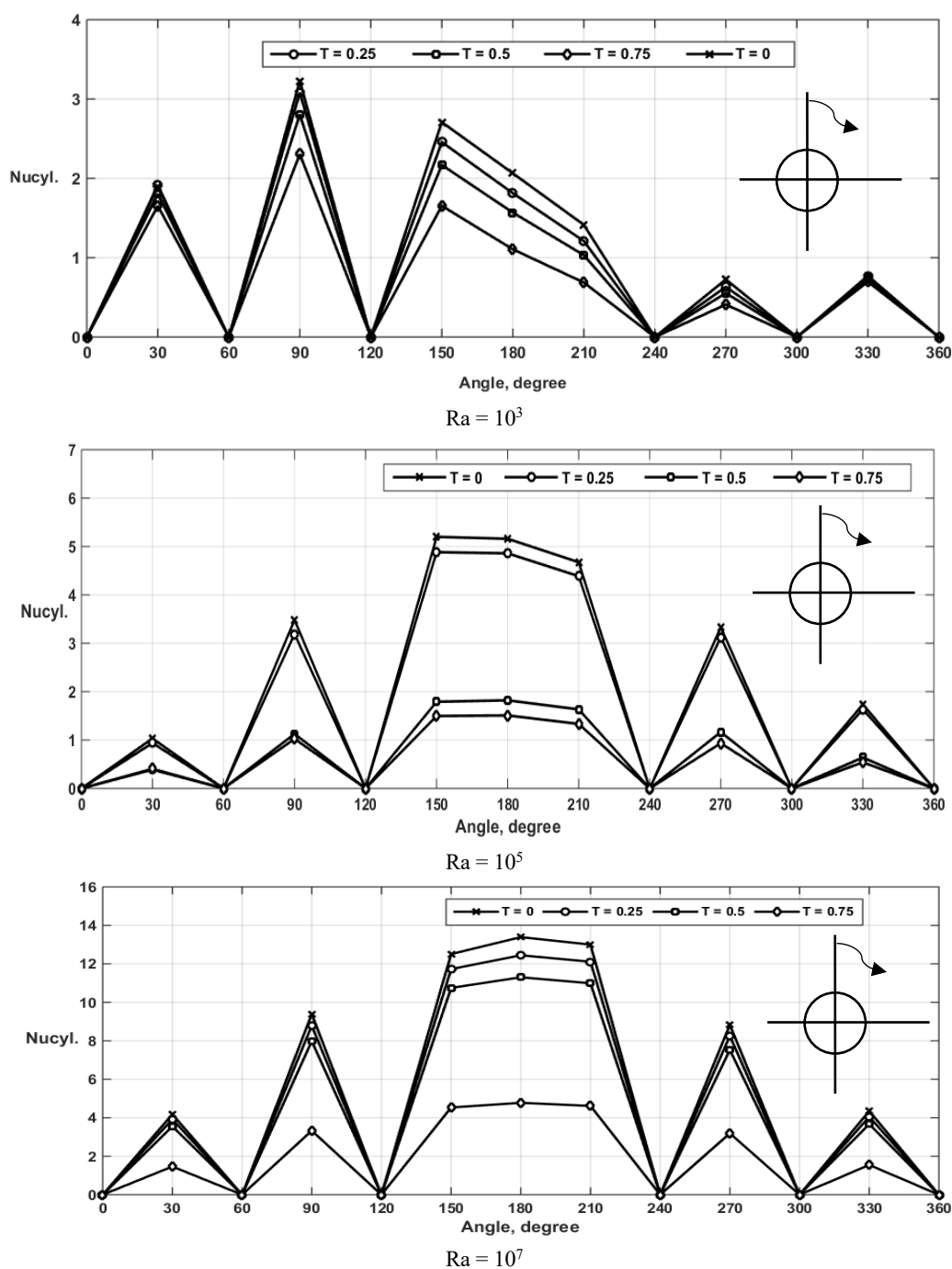


Fig. 9 Localized Nusselt Number around the circular cylinder under various T_r and Ra

5.4 Mean Fluid Temperature and Average Nusselt number

The effects of Ra on the average Nu and mean fluid temperature (T_f) for various dimensionless T_r are presented Fig. 10(a) and Fig. 10(b), respectively. It is evident that Nu has been increased with rising in Ra for all T_r values due to enhance the actions of convective resulting from enhancing the buoyancy force as shown in Fig. 10(a). It has been found that the maximum reduction in average Nu is about 32% when $T_r = 0.75$ as compared to those obtained when $T_r = 0$. The dimensionless fluid temperature T_f has been reduced with increasing in Ra for $T_r = 0$. Similar behavior has been observed for $T_r = 0.25$ and $T_r = 0.5$. On the other hand, the behavior of T_f has been found to be approximately

constant when $T_r = 0.75$. Such issue can be explained by that the temperature difference between cylinder and right wall temperature is reduced. The impact of T_r on Nu and T_f for various Ra are presented in Fig. 10(c) and Fig. 10(d), respectively. The solutions illustrate that Nu has been decreased with rising in Ra for all cases. However, the reduction rate becomes very small for low Ra as displayed in Fig. 10(c). Figure 10(d) displays the variations of T_f with respect to T_r for various Ra , where the solutions show that T_f has been increased with increasing in T_r for all Ra . As Ra is reduced, T_f has been raised, where the enhancement in T_f becomes very small for low Ra .

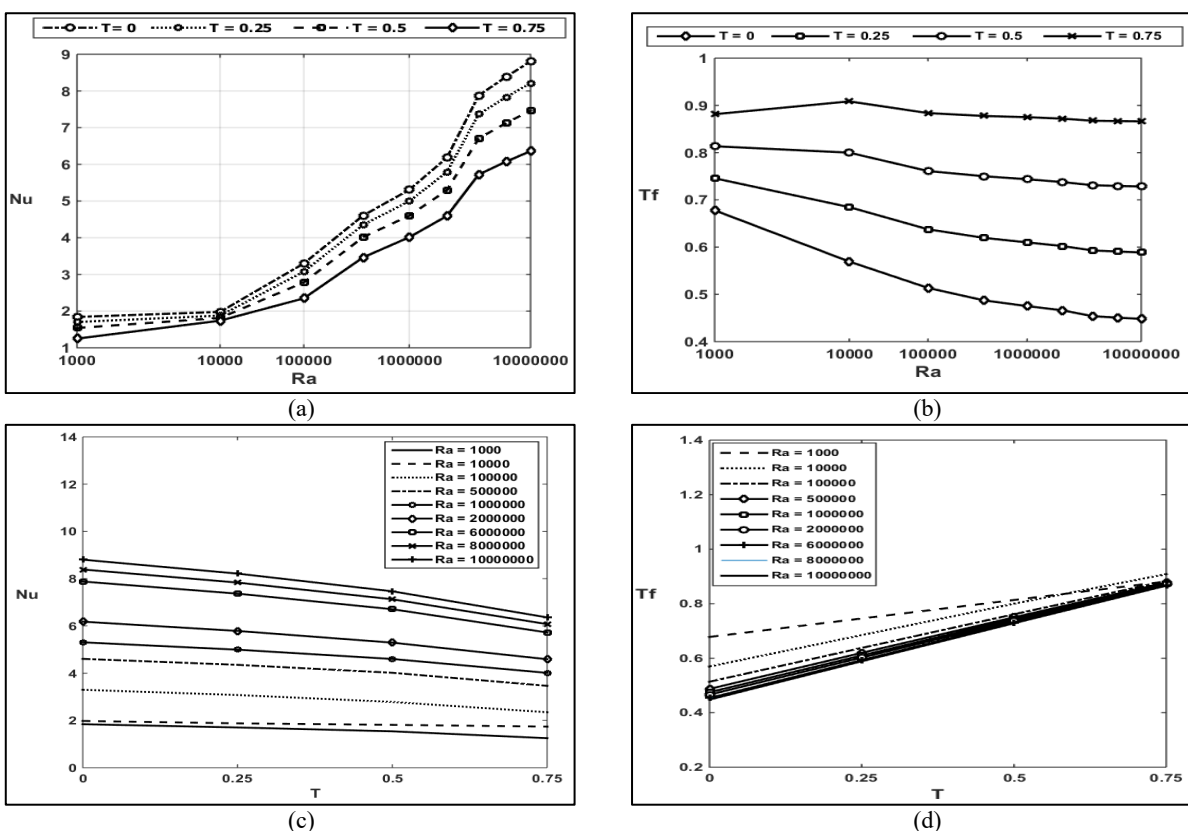


Fig. 10 Variations of (a) Nu for different T_r , (b) T_f for different T_r , (c) Nu for different Ra and (d) T_f for different Ra

6. CONCLUSIONS

The current study includes a numerical investigation on natural convection heat transfer induced from heated cylinder immersed inside enclosed duct cooled from one side. The surfaces of the enclosure have been well insulated except the right vertical surface has been subjected with different cold temperature (T_r). Navier-Stokes and energy equations have been used to display the structures of flow and heat fields. The formulations have been solved utilizing ANSYS FLUENT (version 16.1). The simulations have been done for a large range of Rayleigh number (Ra) and dimensionless right wall temperature (T_r), ranging from 10^3 to 10^7 and from 0 to 0.75, respectively. The present numerical solutions have been compared with previous numerical study and they show a good matching between them. The outcomes of isotherms, streamlines, local Nusselt number (Nu_{cyl}), average Nusselt number (Nu) and fluid temperature (T_f) have been illustrated. The next outcomes are set from the current study:

- The findings display that the activity of natural convection reduces with increasing in T_r , where the peak reduction in Nu is nearly equal 32% for $T_r=0.75$ as compared to $T_r=0$.
- The value of Nu considerably decreases with rising in T_r and decreasing in Ra . In addition, the value of T_f increases with increasing in T_r and its decreases with increasing in Ra .
- For low Ra value, the outcomes illustrate that the change in T_r has a very little action on the behavior of streamlines and a large impact on isotherms contour lines.
- The findings illustrate that the peak Nu_{cyl} is obtained at right side of the cylinder (i.e., at 90°). The change in local Nu_{cyl} with the changing in the value of T_r is high in the region between 120° and 240° . Results also display that Nu_{cyl} values for $T_r=0$ and 0.25 are larger than those when $T_r=0.5$ and 0.75.

- The findings display that the hydrodynamic and thermal boundaries layers thickness around the circular cylinder have been increased as T_r is increased. The upwelling plume has been appeared above the cylinder at $T_r=0$. The variation of Nu_{cyl} at $Ra=10^4$ show that the maximum values of Nu_{cyl} have been located below the cylinder surface at the angles between 150° and 210° .
- The behaviors of thermal and flow structures are completely differ for high Ra values in comparison low Ra values due to the effect of buoyancy force.
- The thermal plume width and the thermal layer thickness have been decreased as Ra is raised. As T_r is increased, the width of upwelling plume and the thickness of thermal boundary have been increased.
- The solutions of Nu_{cyl} display that Ra has an extremely actions on the flow and heat fields.

A final remark, the numerical work that deals with the present topic by filling the cavity with porous medium is very rear and it has been involved only without adding heated single/multi cylinder. The filling the duct by porous structure along with heated cylinder can improve the rate of heat transfer. Consequently, to progress the current study, prospective study must implement a numerical investigation on natural convection induced from hot cylinder immersed in closed porous duct cooled from side. This outcomes are needed to understand the existence of no-slip conditions close to the duct walls and to have further insight on the characteristics of heat transfer. This issue will be considered in the future as a new study. In addition, the experiment works related to this topic by involving porous media inside the cavity is too limited and it was performed only without including heated cylinder in a porous duct. Generally, the size, number and locations of heated pipe can affect the solutions. Thus, to further progress this work, prospective work must implement an experiment investigation on natural convection induced from heated single/multi cylinder inserted inside porous ducted. The outcomes are necessary to verify the numerical solutions. Moreover, the measurement of velocity will use to explain the existence of no-slip

conditions close to duct walls. Also, this issue will be assumed in the future as a new work.

NOMENCLATURE

d	cylinder diameter, m
g	Gravitational acceleration, m/s^2
h	Heat transfer coefficient for air, $W/m^2 K$
k	Thermal conductivity of air, $W/m K$
Nu	Nusselt number
P	Dimensionless pressure
Ra	Rayleigh number
Re	Reynolds number
Ri	Richardson number
s	Spacing size between two cylinders, m
S	Dimensionless spacing size between two cylinders
T	Dimensionless Temperature, $^{\circ}C$
u	Axial velocity, m/s
v	Transverse velocity, m/s
U	Dimensionless velocity in x-direction
V	Dimensionless velocity in y-direction
x	Dimensional axial coordinate, m
y	Dimensional transverse coordinate, m
X	Dimensionless axial coordinate
Y	Dimensionless transverse coordinate
Greek letters	
α	Thermal diffusivity, m^2/s
β	Volumetric thermal expansion coefficient, K^{-1}
μ	Dynamic viscosity, $kg/m s$
ρ	Air density, kg/m^3
Subscripts	
av	Average
eff	Effective
e	Enclosure
c	Cylinder surface
R	Right
F	Fluid

References

Ali, O., Zaidky, R., Saleem, A., 2014, "Numerical Investigation of Natural Convection Heat Transfer from Circular Cylinder inside an Enclosure Containing Nanofluids", *International journal of Mechanical Engineering and Technology*, 5(12), 66–85.

Ali, O. M., Mahmood, R. A., 2020, "Effect of Radiation on Natural Convection Heat Transfer from Heated Horizontal Cylinder in Vented Enclosure", *IOP Conf. Ser. Mater. Sci. Eng.*, 978, 012030. <https://dx.doi.org/10.1088/1757-899X/978/1/012030>

Ali, O. M., Mahmood, R. A., Brifkani, M., 2022, "Augmentation of Convection Heat Transfer from A Horizontal Cylinder in A Vented Square Enclosure with Variation of Lower Opening Size", *Therm. Sci.*, 26 (3), 2027-2041. <https://doi.org/10.2298/TSCI201119176A>

Ali, O., 2014, "Numerical Investigation of Prandtl Number Effects on The Natural Convection Heat Transfer from Circular Cylinder in an Enclosed Enclosure", *Sci. J. Univ. Zakho*, 2 (2), 358–374. <https://www.sjuoz.uoz.edu.krd/index.php/sjuoz/article/view/256> (Accessed: 4 April 2023).

Ali, O., Experimental and Numerical Investigation of Natural Convection Heat Transfer from Different Cross Section Cylinders in a Vented Enclosure, PhD Thesis, Mosul University, 2008.

Ali, O. M., Alomar, O. R., 2021, "Mixed convection heat transfer from two aligned horizontal heated cylinders in a vented square enclosure", *Therm. Sci. Eng. Prog.*, 25, 101041. <https://dx.doi.org/10.1016/j.tsep.2021.101041>

Alomar, O. R., Saeed, R. H., Ali, O. M., 2023, "Impacts of Size and Location of Outflow Opening Vent on Mixed Convective Heat Transfer Induced by Two Aligned Heated Cylinders Immersed in a Partially Open Channel", *Heat Transfer*. <https://dx.doi.org/10.1002/hjt.22823>

ANSYS, I., 2018, "ANSYS Fluent Tutorial Guide R18", ANSYS Fluent Tutor. Guid. 18, no. April, 724–746.

Al-Jabair, S., Habeeb, L. J., 2012, "Simulation of natural convection in concentric annuli between an outer inclined square enclosure and an inner horizontal cylinder, World Academy of Science", *Engineering and Technology*, 69. <https://dx.doi.org/10.5281/zenodo.1327837>

Atayılmaz, Ş. Ö, Teke, İ., 2009, "Experimental and numerical study of the natural convection from a heated horizontal cylinder", *International Communications in Heat and Mass Transfer*, 36, 731 – 738. <https://dx.doi.org/10.1016/j.icheatmasstransfer.2009.03.017>

Billah, M.M., Rahman, M.M., Uddin M. Sharif, N.A. Rahim, R. Saidur, Hasanuzzaman, M., 2011, "Numerical analysis of fluid flow due to mixed convection in a lid-driven cavity having a heated circular hollow cylinder", *International Communications in Heat and Mass Transfer*, 38, 1093 – 1103. <https://dx.doi.org/10.1016/j.icheatmasstransfer.2011.05.018>

Hussain, S. H., Hussein, A. K., 2011, "Natural convection heat transfer in a differentially heated square enclosure with a heat generating-conducting circular cylinder at different diagonal locations", *6th International Advanced Technologies Symposium (IATS'11)*, 16-18, Elazığ, Turkey.

Ganesh, G. R., Sridhar, W., 2021, "Numerical Approach Of Heat And Mass Transfer Of Mhd Casson Fluid Under Radiation Over An Exponentially Permeable Stretching Sheet With Chemical Reaction And Hall Effect", *Frontiers in Heat and Mass Transfer (FHMT)*, 16(5). <http://dx.doi.org/10.5098/hmt.16.5>

Ghaddart, N. K., 1992, "Natural convection heat transfer between a uniformly heated cylindrical element and its rectangular enclosure", *Int. J. Heat Mass Transfer*. 35 (10), 2327 – 2334. [https://dx.doi.org/10.1016/0017-9310\(92\)90075-4](https://dx.doi.org/10.1016/0017-9310(92)90075-4)

Kim, M., Doo, J. H., Park, Y. G., Yoon, H. S., Ha, M. Y., 2014, "Natural convection in a square enclosure with a circular cylinder according to the bottom wall temperature variation", *Journal of Mechanical Science and Technology*, 28 (12), 5013-5025. <https://dx.doi.org/10.1007/s12206-018-0623-9>

Kim, M., Doo, J. H., Park, Y. G., Yoon, H. S., Ha, M. Y., 2014, "Natural convection in a square enclosure with a circular cylinder according to the bottom wall temperature variation", *J. Mech. Sci. Technol.*, 28 (12), 5013–5025. <https://dx.doi.org/10.1007/s12206-014-1123-1>

Karimi, F., Xu, H., Wang, Z., Yang, M., Zhang, Y., 2016, "Numerical simulation of steady mixed convection around two heated circular cylinders in a square enclosure", *Heat Transf. Eng.*, 37 (1), 64–75. <https://dx.doi.org/10.1080/01457632.2015.1042343>

Kuscu, H., Kahveci, K., Tulu Tanju, B., 2015, "Natural convection in a square enclosure cooled by peltier effect", *Proc. World Congr. Mech. Chem. Mater. Eng.*, 315, 20–21.

Kahwaji, G. Y., Hussien, A. S., Ali, O. M., 2012, "Numerical investigation of natural convection heat transfer from square cylinder in a vented enclosure", *Appl. Mech. Mater.*, 110–116, 4451–4464. <https://dx.doi.org/10.4028/www.scientific.net/AMM.110-116.4451>

Kahwaji, G. Y., Hussien, A. S., Ali, O. M., 2011, "Experimental Investigation of Natural Convection Heat Transfer From Rhombic Cross Section Cylinder in a Vented Enclosure", *J. Polytech.*, 1 (1).

Kahwaji, G. Y., Hussien, A. S., Ali, O. M., 2013, "Experimental Investigation Of Natural Convection Heat Transfer From Square Cross Section Cylinder In A Vented Enclosure", *J. Univ. DUHOK Pure Eng. Sci.*, 16 (1).

<https://dx.doi.org/10.26682/eissn.2521-4861>

Nagalakshmi, P.S.S., Vijaya, N., 2022, "Entropy generation of three dimensional Bingham Nanofluid flow with carbon nanotubes passing through parallel plates", *Frontiers in Heat and Mass Transfer (FHMT)*, 19, 17.

<http://dx.doi.org/10.5098/hmt.19.17>

Nabavizadeh, S. A., Talebi, S., Sefid, M., Nourmohammadzadeh, M., 2012, "Natural convection in a square cavity containing a sinusoidal cylinder", *Int. J. Therm. Sci.*, 51 (1) 112–120.

<https://dx.doi.org/10.1016/j.ijthermalsci.2011.08.021>

Nada, S. A., Said, M. A., 2019, "Effects of fins geometries, arrangements, dimensions and numbers on natural convection heat transfer characteristics in finned-horizontal annulus", *Int. J. Therm. Sci.*, 137, 121–137.

<https://dx.doi.org/10.1016/j.ijthermalsci.2018.11.026>

Shu, C., Zhu, Y. D., 2002, "Efficient computation of natural convection in a concentric annulus between an outer square cylinder and an inner circular cylinder", *Int. J. Numer. METHODS FLUIDS*, 38, 429–445.

<https://doi.org/10.1002/flid.226>

Sravanthi, P.M., Madhavi, M.R., 2022, "Nanofluid Flow in Presence of Gyrotactic Microorganisms on the Stretching Surface With Magnetic Field and Activation Energy", *Frontiers in Heat and Mass Transfer*, 19, 19.40.

<https://dx.doi.org/10.5098/hmt.19.40>

Saleh, H., Alsabery, A. I., Hashim, I., 2015, "Natural convection in polygonal enclosures with inner circular cylinder", *Advances in Mechanical Engineering*. 7 (12), 1–10.

<https://dx.doi.org/10.1177/1687814015622899>

Sheikholeslami, M., Gorji-Bandpy, M., Ganji, D. D., Soleimani, S., Seyyedi, S. M., 2012, "Natural convection of nanofluids in an enclosure

between a circular and a sinusoidal cylinder in the presence of magnetic field", *International Communications in Heat and Mass Transfer*, 39, 1435 – 1443.

<https://dx.doi.org/10.1016/j.icheatmasstransfer.2012.07.026>

Sheikholeslami, M., Ellahi, R., Hassan, M., Soleimani, S., 2014, "A study of natural convection heat transfer in a nanofluid filled enclosure with elliptic inner cylinder", *International Journal of Numerical Methods for Heat & Fluid Flow*, 24 (8), 1906 – 1927.

<https://dx.doi.org/10.1108/HFF-07-2013-0225>

Sheikholeslami, M., Hashim, I., Soleimani, S., 2013, "Numerical investigation of the effect of magnetic field on natural convection in a curved-shape enclosure", *Mechanical Problems in Engineering*, 2013, 831725.

<https://dx.doi.org/10.1155/2013/831725>

Shu, C., Xue, H., Zhu, Y. D., 2001, "Numerical study of natural convection in an eccentric annulus between a square outer cylinder and a circular inner cylinder using DQ method", *Int. J. Heat Mass Transf.*, 44 (17), 3321–3333.

[https://dx.doi.org/10.1016/S0017-9310\(00\)00357-4](https://dx.doi.org/10.1016/S0017-9310(00)00357-4)

Talesh Bahrami, H. R., Safikhani, H., 2020, "Heat transfer enhancement inside an eccentric cylinder with an inner rotating wall using porous media: a numerical study", *J. Therm. Anal. Calorim.* 141, 1905–1917.

<https://dx.doi.org/10.1007/s10973-020-09532-y>

Webb, S. W., Itamura, M. T., Francis, N. D., James, D. L., 2003, "CFD calculation of internal natural convection in the annulus between horizontal concentric cylinders", *Proc. ASME Summer Heat Transf. Conf.*, 2003, 911–916.

<https://dx.doi.org/10.1115/ht2003-47515>

Yoon, H. S., Shim, Y. J., 2021, "Classification of flow modes for natural convection in a square enclosure with an eccentric circular cylinder", *Energies*, 14 (10), 2788.

<https://dx.doi.org/10.3390/en14102788>